Measuring ^{19}F Shift Anisotropies and ^{1}H – ^{19}F Dipolar Interactions with Ultrafast MAS NMR

Francesca Martini§, Habeeba K. Miah†, Dinu Iuga‡, Marco Geppi§ and Jeremy J. Titman†*

§*Dipartimento di Chimica e Chimica Industriale, Università di Pisa, Via Giuseppe Moruzzi 3, 56124 Pisa, Italy*

†*School of Chemistry, University of Nottingham, University Park, Nottingham, NG7 2RD, UK*

‡*UK 850 MHz Solid-state NMR Facility, Department of Physics, Millburn House, University of Warwick, Coventry, CV4 7AL, UK*

**Corresponding author: Email: Jeremy.Titman@nottingham.ac.uk, Tel: +44 115 951 3560*

Abstract

A new ^{19}F anisotropic-isotropic shift correlation experiment is described that operates with ultrafast MAS, resulting in good resolution of isotropic ^{19}F shifts in the detection dimension. The new experiment makes use of a recoupling sequence designed using symmetry principles that reintroduces the ^{19}F chemical shift anisotropy in the indirect dimension. The situations in which the new experiment is appropriate are discussed, and the ^{19}F shift anisotropy parameters in poly(difluoroethylene) (PVDF) are measured. In addition, similar recoupling sequences are shown to be effective for measuring ^{1}H – ^{19}F distances via the heteronuclear dipolar interaction. This is demonstrated by application to a recently synthesized zirconium phosphonate material that contains one-dimensional chains linked by H – F hydrogen bonds.

Keywords: chemical shift anisotropy, ultrafast magic angle spinning, anisotropic-isotropic shift correlation, symmetry-based recoupling sequence, heteronuclear dipolar coupling, dipole-shift correlation.

Introduction

Measurements of chemical shift parameters in solids for abundant nuclei like ^{1}H and ^{19}F are challenging, because of the effects of strong homonuclear dipolar couplings, and for ^{1}H the difficulties are compounded by the relatively small ^{1}H chemical shift anisotropy (CSA). Nevertheless, several methods for measuring ^{1}H shift parameters in solids have been demonstrated recently, based on two-dimensional magic angle spinning (MAS) experiments that correlate the anisotropic and isotropic parts of the shift interaction. These distinguish the different ^{1}H sites in the detection dimension and reintroduce or "recouple" the MAS-

averaged ^{1}H CSA during the evolution time. For example, Brouwer and Ripmeester[1] resolved the ^{1}H isotropic shifts in ν_2 by a combination of moderate MAS ($\omega_r/2\pi$ = 16 kHz) and multi-pulse homonuclear decoupling and used a recoupling sequence designed using symmetry principles[2,3] during t_1. Hou *et al.*[4] optimized the resolution of ^{1}H sites by magnetization transfer to a neighbouring ^{15}N nucleus after recoupling the ^{1}H CSA in a similar fashion and measured the ^{1}H shift anisotropy parameters for the amide sites in ^{15}N-enriched proteins. Miah *et al.*[5] employed modified recoupling sequences suitable for use with "ultrafast" MAS ($\omega_r/2\pi$ > 50 kHz), an approach that allows hydrogen-bonded sites in simple crystalline solids to be resolved in ν_2 without the need for multi-pulse homonuclear decoupling. Duma *et al.*[6] used a similar method but with rotary resonance in ν_1.

Resolution in ^{19}F spectra of solids can be similarly compromised by strong homonuclear dipolar interactions, but the range of chemical shifts observed for ^{19}F is significantly greater than for ^{1}H. In principle, the combination of fast MAS and spinning sideband analysis[7] allows the extraction of the shift parameters, especially when the CSA is large or at high B_0 field. However, as noted previously,[8,9] the MAS rate required to average the dipolar interactions is often so large that the spinning sideband intensities are low. Hence, measurements of the ^{19}F shift parameters in powders often rely on multiple-pulse homonuclear decoupling,[10] but this approach can be complicated by overlap between CSA powder patterns that result from different ^{19}F sites. In this communication, we demonstrate an alternative approach that is particularly suitable for systems containing several inequivalent ^{19}F nuclei. This is based on a ^{19}F anisotropic-isotropic shift correlation experiment that utilizes a symmetry-based recoupling sequence optimized for use with ultrafast MAS. We illustrate the utility of the new experiment by measurements of the ^{19}F shift parameters in poly(difluoroethylene) (PVDF). The recoupling sequences also reintroduce heteronuclear dipolar couplings, and we consider the effect of these on the recoupled ^{19}F CSA lineshape, showing that ^{1}H – ^{19}F interactions can be neglected for the case of PVDF. Finally, we demonstrate that ^{1}H – ^{19}F dipolar couplings can be more effectively measured using similar recoupling sequences applied to the ^{1}H channel only. This is demonstrated by a study of a recently synthesized zirconium phosphonate material that contains one-dimensional chains linked by H – F hydrogen bonds.

Pulse Sequence Design

Levitt and co-workers[2,3] applied symmetry principles to the design of recoupling sequences that reintroduce specific nuclear spin interactions averaged by MAS. This work makes use of the most flexible class of symmetry-based recoupling sequences, designated $\mathrm{R}N_n^\nu$, which consist of N composite inversion pulses R, timed to occupy n rotor periods. Each R element of the overall sequence has duration $n\tau_r/N$ and alternate elements have phases $\pm\pi\nu/N$. It has been shown[2] that the symmetry numbers N, n and ν determine which interactions are retained in the first-order effective Hamiltonian for the sequence according to:[11]

$$H_{lm\lambda\mu}^{(1)}(t_0) = \kappa_{lm\lambda\mu} A'_{lm} \exp\left\{-im\left(\alpha_{RL}^0 - \omega_r t_0\right)\right\} T_{\lambda\mu} \text{ if } \left(nm - \nu\mu\right) = \frac{N}{2} k_\lambda \qquad (1)$$

where A' is a rank-l irreducible spherical tensor operator describing the spatial part of the interaction Hamiltonian in the rotor frame, and T is a rank-λ irreducible spherical tensor operator describing the spin part in the laboratory frame. The rotational components of the spatial and spin tensors m and μ take values m = l, l - 1, … -l and μ = λ, λ - 1, … - λ, respectively, and k_λ is any integer with the same parity as λ. The scaling factor $\kappa_{lm\lambda\mu}$ describes the reduction in magnitude of the symmetry-allowed interaction that is an inevitable consequence of recoupling, and the Euler angle α_{RL}^0 describes the orientation of the rotor with respect to the laboratory frame at time t_0.

Recoupling sequences suitable for measuring shift parameters result in a transverse single-quantum Hamiltonian that takes the form

$$H^{(1)} = \sum_j \left(\omega_j T_{1-1} + \omega_j^* T_{11}\right) \qquad (2)$$

to first order, where the index j runs over all chemical shift interactions. The coefficients ω_j depend on the spatial part of the chemical shift interaction, as well as the scaling factor. Suitable sequences must avoid inadvertently recoupling the homonuclear dipolar interaction and the isotropic shift, while first-order compensation for rf amplitude inhomogeneity can also be included.[11] Many symmetries fit these criteria, including $\mathrm{R}18_2^5$, $\mathrm{R}12_1^4$ and $\mathrm{R}16_3^2$, but several additional factors must be considered when selecting a recoupling sequence to measure ^{19}F shift parameters. Ultrafast MAS is particularly appropriate in the ^{19}F case, since in this way a well-resolved isotropic spectrum can be acquired in the direct dimension without the need for homonuclear decoupling. However, the pulse sequence is synchronized with the spinning, so that many symmetries requiring a large ratio ω_1/ω_r become impractical at higher MAS rates. For example, $\mathrm{R}18_2^5$ and $\mathrm{R}12_1^4$ require rf amplitudes in excess of 180 kHz and 240 kHz, respectively, for MAS rates above

40 kHz. In addition, for relatively large ^{19}F shift anisotropies the dwell time in t_1 must be short to avoid aliasing of the broad CSA patterns that are recoupled. For a given symmetry larger ω_r results in a shorter dwell time, but, as shown below, ultrafast MAS alone is often insufficient to provide the necessary expansion of the spectral width in the indirect dimension in the ^{19}F case. One solution is to make use of a recoupling sequence with a low scaling factor. According to Hou *et al.*[12] this can be achieved by selection of a low ratio N/n which in turn results in a low ω_1/ω_r factor suitable for ultrafast MAS. An alternative approach involves using a dwell time that is shorter than the cycle time for a complete $\mathrm{R}N_n^\nu$ sequence. Sampling the indirect dimension in this way results in the appearance of cycling sidebands that must remain outside the recoupled powder pattern to avoid spectral distortion. In practice a combination of the two approaches is appropriate, and in this work ^{19}F isotropic-anisotropic correlation spectra have been recorded with a $\mathrm{R}12_5^4$ sequence. This benefits from a low scaling factor of 0.155 and fairly modest rf requirements with $\omega_1/\omega_r = 1.2$ which should be compared with corresponding values of $\kappa_{lm\lambda\mu} = 0.279$ and $\omega_1/\omega_r = 2.667$ for $\mathrm{R}16_3^2$.

In the interaction frame of a single resonant rf field the rotational components of the spin and spatial parts of the heteronuclear dipolar coupling are identical to those for the CSA. Therefore, all the $\mathrm{R}N_n^\nu$ symmetries described above reintroduce the heteronuclear dipolar coupling in addition to the ^{19}F CSA, apparently making the method unsuitable for measuring ^{19}F shift parameters in the presence an abundant heteronucleus, such as ^{1}H. One solution to this problem is to apply the recoupling sequence simultaneously to both the ^{19}F and ^{1}H channels.[13] However, in practice this is often not necessary for ^{19}F, since the large CSA dominates the recoupled lineshape, especially at high B_0 field, and this is demonstrated to be the case for the PVDF. For the same reason measurements of the ^{1}H – ^{19}F dipolar coupling are more effectively made using similar recoupling sequences applied to the ^{1}H channel because of the relatively small size of the ^{1}H CSA. Experiments of this type have been demonstrated previously for ^{1}H – ^{13}C and ^{1}H – ^{15}N interactions in proteins by Hou *et al.*[12]

Experimental

The pulse sequence used to record ^{19}F anisotropic-isotropic shift correlation spectra has been described previously in Ref. [5]. As discussed above, a $\mathrm{R}12_5^4$ recoupling sequence is more appropriate in the ^{19}F case than the $\mathrm{R}16_3^2$ alternative used in that work for ^{1}H. Experiments were recorded at a ^{19}F Larmor frequency of 564.7 MHz, using a double-resonance 1.3 mm MAS probe. MAS rates of 65.0 kHz were selected, so that the

$R12_5^4$ recoupling sequence required a ^{19}F rf amplitude of 78.0 kHz. Further experimental details are given in the relevant figure caption. A schematic describing all the processing steps for the ^{1}H case was included in Ref. [5] and a similar procedure was employed here. ^{1}H – ^{19}F heteronuclear dipolar couplings were measured using a ^{1}H variant of the anisotropic-isotropic shift correlation experiment recorded at a Larmor frequency of 600.13 MHz. The MAS rate was 62.5 kHz, and a $R16_3^2$ recoupling sequence was used requiring a ^{1}H rf amplitude of 166.6 kHz. Further experimental details are given in the relevant figure caption. Additional ^{1}H decoupled ^{19}F MAS spectra were recorded at a ^{19}F Larmor frequency of 800 MHz and a spinning rate of 25 kHz using a 2.5 mm triple-resonance (HFX) probe.

The anisotropy and asymmetry parameters for the chemical shift are defined according to $\zeta = \delta_{zz} - \delta_{iso}$ and $\eta = (\delta_{yy} - \delta_{xx})/\zeta$, respectively, with the principal components ordered according to $|\delta_{zz} - \delta_{iso}| \geq |\delta_{xx} - \delta_{iso}| \geq |\delta_{yy} - \delta_{iso}|$. Numerical simulations of the recoupled ^{19}F CSA lineshapes were performed using SIMPSON.[14] Powder averaging was achieved using 615 (α,β) orientations chosen according to the scheme of Zaremba[15] and 5 uniformly distributed values of γ. Where appropriate B_1 inhomogeneity was included by summing 13 simulations carried out using rf amplitudes weighted according to the experimentally determined B_1 distribution, as described in Ref. [5].

To extract the ^{19}F CSA an array of these simulated lineshapes was generated for a suitable range of ζ values and η between 0.0 to 1.0, and the ^{19}F shift anisotropy parameters were extracted by comparing these with the experimental data, using a similar method to that described in Ref. [1]. For each simulated lineshape the optimal scaling was found by fitting to the experimental data, and the corresponding χ^2 parameter was plotted as a function of ζ and η. The resulting error surface allows the best-fit values of ζ and η to be obtained, as well as their confidence limits, assuming χ^2 is suitably normalized.[16] A similar procedure was followed in order to obtain ^{1}H – ^{19}F distances from heteronuclear dipolar couplings measured using a ^{1}H anisotropic-isotropic shift correlation, except that in this case both the ^{1}H shift parameters and the ^{1}H – ^{19}F couplings determine the recoupled lineshape. More details of how the resulting multi-dimensional error surface was explored in the case described here are given below.

Results and Discussion

^{19}F Shift Parameters

To illustrate the problems of measuring ^{19}F shift parameters Figure 1 shows ^{19}F MAS spectra of PVDF recorded at a Larmor frequency of 564.7 MHz. The 65 kHz MAS spectrum (a) contains five well-resolved lines with the most intense peak at -92.0 ppm arising from the amorphous domains of the semi-crystalline PVDF. The peaks at -97.0 and -82.5 ppm have been assigned[17] to the crystalline domains, which in as-polymerized powders contain both α and β polymorphs with tg^+tg^- and all-trans conformations, respectively. Two further peaks are evident around -115 ppm that result from regio-irregular tail-to-tail and head-to-head polymerization.[18] Note that the spectrum in Figure 1(a) closely resembles that recorded previously[19] for a sample containing the pure α form, suggesting that the PVDF powder used in this work contains only a small proportion of the β polymorph.

As discussed above, in principle the ^{19}F CSA can be extracted by analysis of the spinning sidebands observed at more moderate MAS rates. In practice this approach is complicated by the need to balance the conflicting MAS requirements of optimizing spectral resolution and preserving sufficient sidebands for analysis, as well as by overlap between spinning sidebands. This is illustrated in the 25 kHz MAS spectrum (b), which shows a significant decrease in the resolution of the three main isotropic lines between -80 and -100 ppm. Although the ^{19}F shift parameters can be extracted from the spinning sidebands observed at this more moderate MAS rate, these are too few in number for an accurate analysis. Spectra recorded at MAS rates below 25 kHz suffer from overlap between the sidebands and the regio-irregular isotropic peaks around -115 ppm.

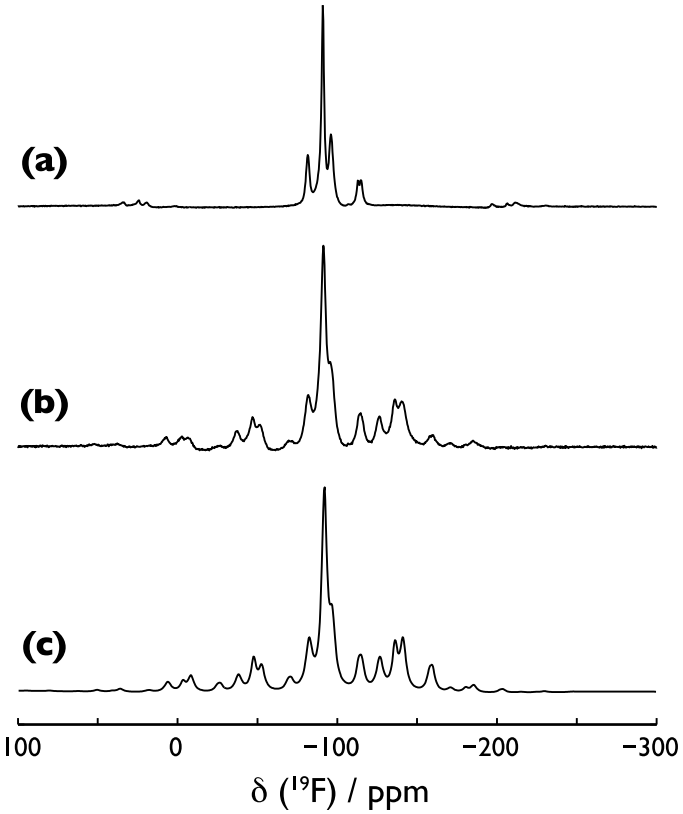

Figure 1. ^{19}F MAS spectra of PVDF, recorded at a Larmor frequency of 564.7 MHz. Experimental spectra for as-polymerized powder at MAS rates of 65 kHz and 25 kHz, respectively, are shown in (a) and (b). These spectra were recorded with 8 scans, using a $\pi/2$ pulse duration of 1.5 μs and a relaxation delay of 2 s. ^{19}F chemical shifts were referenced to CCl_3F. Note the decreased resolution of the isotropic peaks in (b). In addition, (c) shows a simulated spectrum for a MAS rate of 25 kHz calculated using the ^{19}F shift parameters measured from the ^{19}F anisotropic-isotropic shift correlation spectrum in Figure 2. Note the good agreement between experimental and simulated spectra in (b) and (c).

Figure 2(a) shows a ^{19}F anisotropic-isotropic correlation spectrum of as-polymerized powdered PVDF recorded at a Larmor frequency of 564.7 MHz and a MAS rate of 65 kHz using the pulse sequence in Figure 1. Other experimental parameters are given in the caption. Figure 2(b) shows (black lines) cross-sections parallel to ν_1 taken at ν_2 frequencies corresponding to the five isotropic shifts that show lineshapes depending on the recoupled ^{19}F CSA. These are compared with SIMPSON simulations (red dashed lines) for the best-fit ζ and η obtained as described above. The results of the fits are given in Table 1, and the error surfaces with respect to ζ and η are shown in the Supplementary Information (Figure S1). In common with other similar sequences the sign of ζ cannot be determined because of the symmetry of the recoupled CSA lineshape, and in practice the error in η is significant due to the effect of B_1 inhomogeneity (see

Supplementary Information Figure S2). The ^{19}F shift parameters for the two crystalline sites of the α form of PVDF have been measured previously from a $T_{1\rho}$-filtered spectrum recorded with $\omega_r/2\pi$ = 15 kHz.[19] Almost identical shift anisotropies (ζ = 111 and 106 ppm for the lines at δ_{iso} = -82.5 and -97.0 ppm, respectively) were obtained for the two sites, and the agreement with the current values is good. The ^{19}F shift parameters for amorphous PVDF have also been measured previously, in this case from a somewhat distorted spectrum obtained using multiple-pulse homonuclear decoupling.[9] That work gives an estimate of ζ = 41 ppm, and in this case the agreement with the current values is poor. However, it should be noted that the parameters in Table 1 can be used to simulate the ^{19}F MAS spectrum recorded at 25 kHz, as shown in Figure 1. The anisotropic-isotropic correlation spectrum in Figure 2 also allows the ^{19}F shift parameters for the regio-irregular sites to be determined. Previously these sites were shown to be preferentially located in the mobile regions of semi-crystalline PVDF,[19] but the shift parameters in Table 1 are similar to those obtained for the more rigid crystalline sites. This suggests either that the recoupling sequence suppresses the more mobile contributions or that the mobile regions are comparatively dilute in the PVDF powder used in this work.

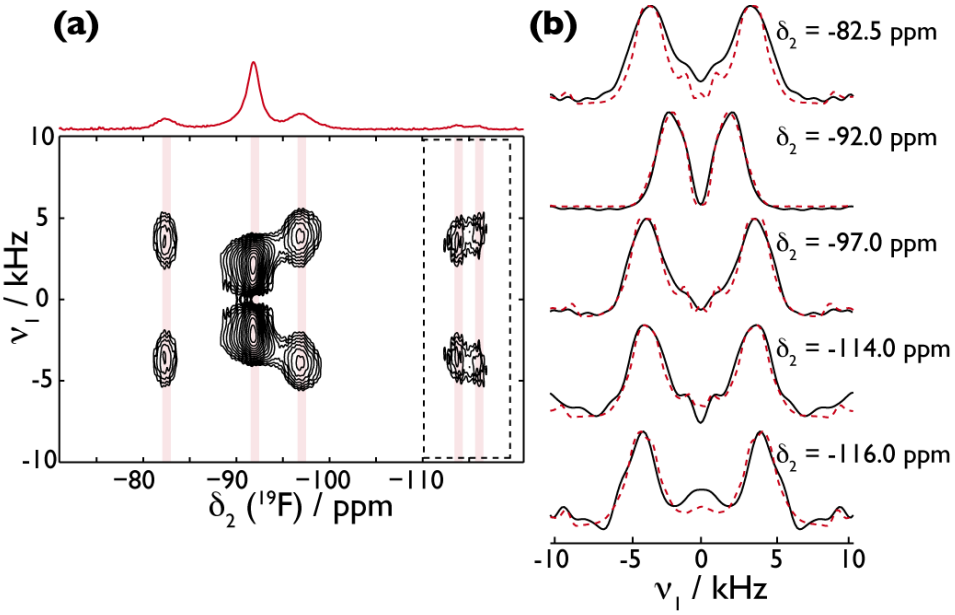

Figure 2. (a) shows a ^{19}F anisotropic-isotropic correlation spectrum of PVDF recorded at a Larmor frequency of 564.7 MHz. The MAS rate was 65 kHz, so that the $R12_5^4$ recoupling sequence required a ^{19}F rf amplitude of 78.0 kHz, corresponding to a π pulse duration of 6.41 μs. There were 32 t_1 increments with data points sampled every 4 R elements, resulting in a dwell time in the indirect dimension of 25.6 μs. In t_2 2048 complex points were acquired with a spectral width of 400 kHz. Saturation was achieved using a train of 200 π/2 pulses separated by intervals of 10 ms with a recovery delay of 10 s. ^{19}F chemical shifts were referenced to CCl_3F. Within the dashed box the contour levels have been raised, so that the less intense response from

regio-irregular tail-to-tail and head-to-head polymers is visible. (b) shows (black lines) cross-sections parallel to ν_1 taken at ν_2 frequencies showing recoupled CSA lineshapes corresponding to the five isotropic ^{19}F shifts, along with SIMPSON simulations (red dashed lines) for the best-fit chemical shift parameters (see Table 1).

The glass transition temperature for PVDF is 240 K, so that at ambient temperature some motional averaging of the ^{19}F CSA can be expected in the amorphous domains, especially given the additional sample heating resulting from ultrafast MAS. These motional effects are responsible for the reduced value of ζ measured for the amorphous line at -92 ppm, but they have not been explicitly included in the lineshape simulations. Using ^{19}F and ^{1}H NMR relaxation studies on crystals of the α form of PVDF McGarvey and Schlick[20] determined that the correlation time for motions about the polymer backbone is much shorter that for rotation about the individual C – C bonds in the chain. As a result ^{1}H – ^{19}F dipolar interactions are not expected to be averaged by chain motion in crystalline PVDF, even with ultrafast MAS. As noted above, RN_n^ν symmetries suitable for measuring the ^{19}F CSA also reintroduce heteronuclear dipolar couplings. For the α form of PVDF the closest H – F contacts are 2.36 Å[21] which corresponds to a ^{1}H – ^{19}F dipolar coupling constant of 8.6 kHz. Figure 3 shows SIMPSON simulations performed as described above of recoupled ^{19}F CSA lineshapes for a ^{19}F – ^{1}H spin pair with shift parameters similar to those obtained for the α form of PVDF, including the effects of B_1 inhomogeneity. In (a) d_{HF} = 8.5 kHz and ζ varies, demonstrating that the recoupled lineshapes are sensitive to the ^{19}F shift anisotropy, since the separation of the maxima in the pattern increases with ζ. In (b) ζ = 105 ppm and d_{HF} varies, suggesting that the ^{1}H – ^{19}F dipolar interaction can be neglected in this case, since the lineshape maxima are unaffected, except for a slight broadening that is largely masked by the effects of B_1 inhomogeneity below d_{HF} = 10 kHz.

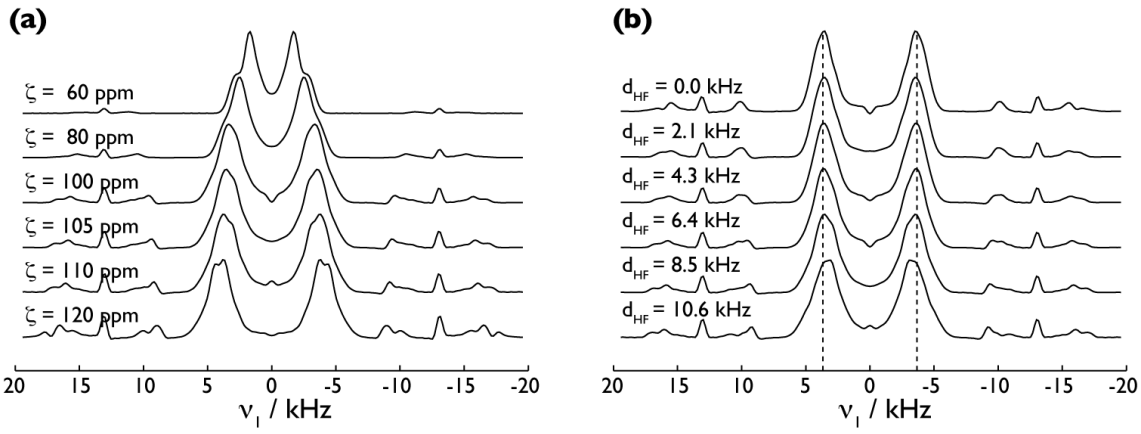

Figure 3. SIMPSON simulations of ^{19}F CSA lineshapes recoupled using a $R12_5^4$ sequence for a ^{1}H – ^{19}F spin pair, with parameters similar to those obtained for the α form of PVDF and including the effects of B_1

inhomogeneity. In (a) d_{HF} = 8.5 kHz and ζ varies, demonstrating that the recoupled lineshapes are sensitive to the ^{19}F CSA, while in (b) ζ = 105 ppm and d_{HF} varies. Apart from a slight broadening that is largely masked by the effects of B_1 inhomogeneity increasing d_{HF} has no effect on the spectrum, suggesting that ^{1}H – ^{19}F dipolar couplings can be neglected in this case. The ^{19}F Larmor frequency was 564.7 MHz, the MAS rate was 65 kHz. The t_1 interferogram was sampled every 4 R elements, resulting in a dwell time of 25.64 μs. In these simulations the B_1 profile was a Gaussian with σ = 8%.

Table 1. Values of ^{19}F chemical shift parameters in PVDF (with 95% confidence limits) measured in this work from fitting to simulated spectra as described in the text.

δ_{iso}[1]	ζ / ppm	η
-82.5	108 ± 10	0.3 ± 0.3
-92.0	68 ± 3	0.5 ± 0.1
-97.0	115 ± 8	0.3 ± 0.3
-114.0	109 ± 8	0.2[2]
-116.0	117 ± 10	0.1 ± 0.2

[1] More precise values for δ_{iso} are given in Ref. [17].

[2] 95% confidence limit for η extends from 0 to 1.

^{1}H – ^{19}F Distances

Since single-channel RN_n^ν sequences reintroduce heteronuclear dipolar couplings in addition to the CSA, they can also be used to measure ^{1}H – ^{19}F dipolar couplings. As discussed above, for ^{19}F the relatively large CSA dominates the recoupled lineshape, and in the case of PVDF the ^{1}H – ^{19}F dipolar interactions can be neglected. Therefore, where the ^{1}H – ^{19}F coupling is the object of the measurement, applying the RN_n^ν sequence to ^{1}H, for which the CSA is an order of magnitude smaller, is a more effective approach. This is illustrated here by a study of hydrogen bonding in a novel zirconium phosphonate with one-dimensional chains of ZrO_3F_3 octahedra and PO_3C tetrahedra.[22] This was synthesized by reacting a novel phosphono-carboxylate ligand made from diethyl 2-bromoethylphosphonic and 4-carboxypyridine (isonicotinic acid) with zirconium in hydrofluoric acid. In the phosphonate (designated sample **1** in Ref. [22]) each carboxylate group of the isonicotinate points toward an adjacent chain with one O atom (O4) only 2.67 Å away from an equatorial F (F2) of a neighbouring ZrO_3F_3 group, suggesting the presence of a H – F hydrogen bond. The hydrogen-bonded H – F contact should correspond to a ^{1}H – ^{19}F dipolar coupling constant of at least 20 kHz which is substantially larger than the ^{1}H CSA at 600 MHz. Figure 4 shows SIMPSON simulations of ^{1}H CSA

lineshapes recoupled using a $R16_2^3$ sequence for a ^{1}H – ^{19}F spin pair, with parameters similar to those expected for the zirconium phosphonate. In (a) the ^{1}H – ^{19}F dipolar coupling is fixed at 20 kHz, while the ^{1}H CSA is allowed to vary from 2 to 25 ppm, while in (b) $\zeta(^1\text{H})$ is fixed at 20 ppm and d_{HF} allowed to vary from 0 to 25 kHz. Clearly, in the ^{1}H case the recoupled lineshapes are sensitive to the ^{1}H – ^{19}F coupling as well as to the ^{1}H shift parameters and can therefore be used to measure H – F distances.

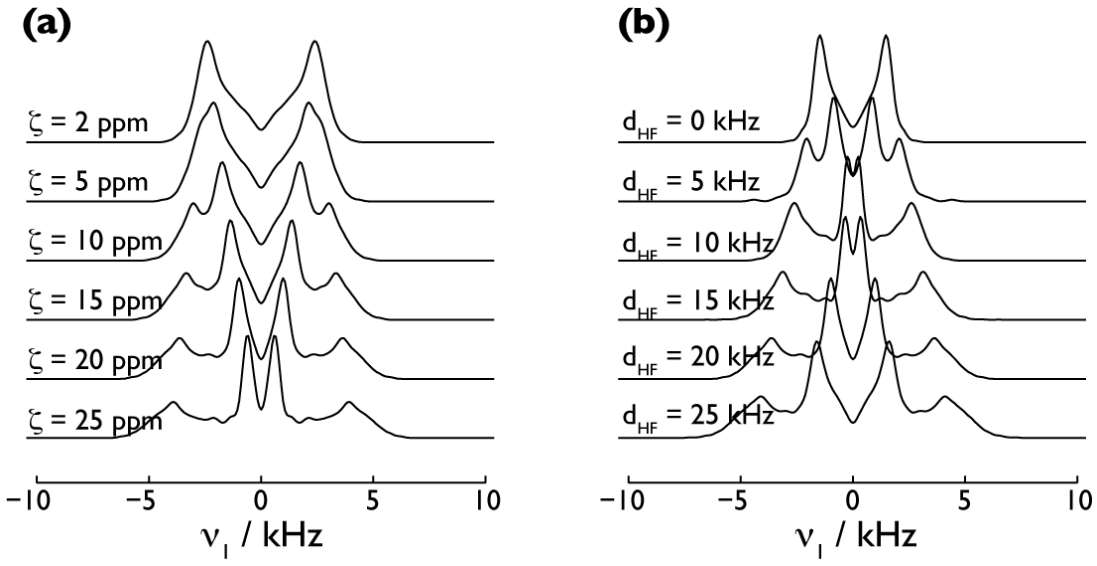

Figure 4. SIMPSON simulations of ^{1}H CSA lineshapes recoupled using a $R16_3^2$ sequence for a ^{1}H – ^{19}F spin pair, with parameters similar to those obtained for the zirconium phosphonate[22] and including the effects of B_1 inhomogeneity. In contrast to the PVDF ^{19}F case for the zirconium phosphonate ^{1}H spectrum the ^{1}H – ^{19}F dipolar couplings cannot be neglected, since they are of comparable size to the ^{1}H CSA. In (a) d_{HF} = 20 kHz and ζ varies, while in (b) ζ = 20 ppm, while the ^{1}H – ^{19}F dipolar coupling varies. These simulations demonstrate that the recoupled lineshapes are sensitive to both the ^{1}H CSA and d_{HF}. The ^{1}H Larmor frequency was 600.13 MHz, and the MAS rate was 62.5 kHz. The t_1 interferogram was sampled every 16 R elements, resulting in a dwell time of 48.0 μs. The B_1 profile was a Gaussian with σ = 8%.

Figure 5(a) shows a ^{1}H anisotropic-isotropic correlation spectrum of the novel zirconium phosphonate recorded at a Larmor frequency of 600.13 MHz and a MAS rate of 62.5 kHz using the $R16_3^2$ sequence introduced in Ref. [5]. Other experimental parameters are given in the caption. The ultrafast MAS ^{1}H spectrum (red) contains several well-resolved resonances, and the deshielded line at 12.5 ppm can be assigned to the H – F hydrogen-bonded ^{1}H site. Figure 5(b) shows (black lines) a cross-section parallel to ν_1 taken at the corresponding ν_2 frequency that shows a lineshape that depends on both the recoupled ^{19}F CSA and the ^{1}H – ^{19}F dipolar coupling. This is compared with a best-fit SIMPSON simulation (red dashed lines),

obtained by exploring the three-dimensional error surface with ^{1}H shift parameters ζ and η, and the position of the hydrogen-bonded H as fit parameters. Cross sections through the three-dimensional error surface are shown in the Supplementary Information (Figure S3). For simplicity the hydrogen-bonded H was constrained to lie on the vector linking the isonicotinate carboxylate O (O4) and the equatorial F (F2) of the neighbouring ZrO_3F_3 group. In addition to the large ^{1}H – ^{19}F dipolar coupling resulting from the hydrogen-bond contact with the equatorial F (F2), two smaller couplings involving the axial F atoms (F1 and F3) were taken into account in the simulations. The fitting results in a hydrogen-bond H – F2 distance of 1.64 Å, corresponding to $d_{H\text{-}F2}$ = 25.50 kHz and ^{1}H shift parameters ζ = 12.4 ppm and η = 0.2. The smaller couplings were $d_{H\text{-}F1}$ = 1.53 kHz and $d_{H\text{-}F3}$ = 2.25 kHz. The consequences of this result for the structure of the zirconium phosphonate will be discussed elsewhere.

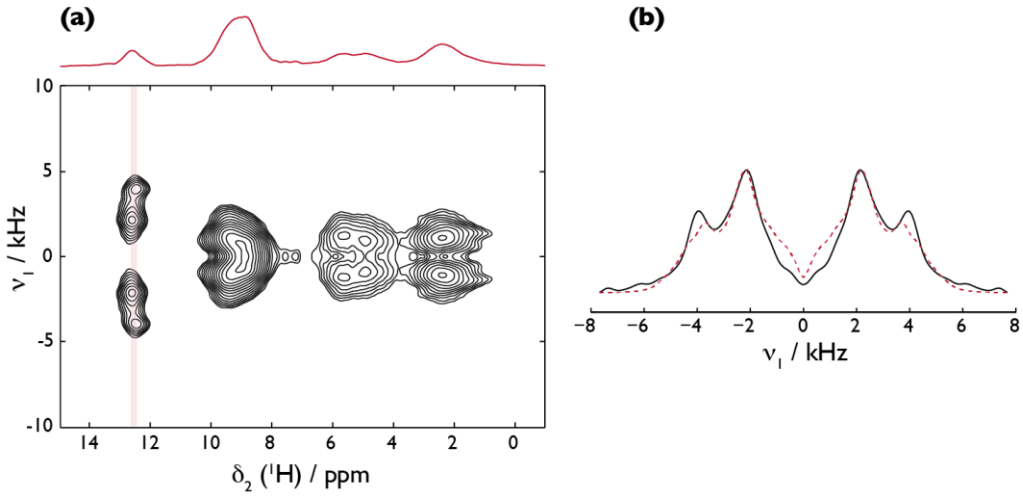

Figure 5. (a) shows a ^{1}H anisotropic-isotropic correlation spectrum of the zirconium phosphonate recorded at a Larmor frequency of 600.13 MHz. The MAS rate was 62.5 kHz, so that the $R16_3^2$ recoupling sequence required a ^{1}H rf amplitude of 166.7 kHz, corresponding to a π pulse duration of 3.0 μs. There were 32 t_1 increments with data points sampled every 16 R elements, resulting in a dwell time in the indirect dimension of 48.0 μs. In t_2 1024 complex points were acquired with a spectral width of 150 kHz. Saturation was achieved using a train of 200 $\pi/2$ pulses separated by intervals of 10 ms with a recovery delay of 30 s. ^{1}H chemical shifts were referenced to TMS. (b) shows a (black line) cross-section parallel to ν_1 taken at the ν_2 frequency of the hydrogen-bonded ^{1}H site at δ_{iso} = 12.5 ppm along with a SIMPSON simulation (red dashed line) for the best-fit parameters, including both the ^{1}H chemical shift and the ^{1}H – ^{19}F dipolar coupling.

For the zirconium phosphonate the ^{19}F CSA (around 200 ppm) is significantly larger than for PVDF, and a 25 kHz ^{19}F MAS spectrum contains plenty of spinning sidebands to analyse for an accurate measurement of the

shift parameters (See Supplementary Information Figure S4). In addition, ^{1}H decoupling can be applied to remove the effects of the substantial ^{1}H – ^{19}F dipolar coupling from the spectrum. In this regime the ^{19}F anisotropic-isotropic shift correlation discussed here is not the most appropriate method to measure the ^{19}F shift parameters.

Conclusion

A new ^{19}F anisotropic-isotropic shift correlation experiment was described that operates with ultrafast MAS, resulting in good resolution of isotropic shifts in the detection dimension, especially in combination with relatively high B_0 fields. A recoupling sequence is required to reintroduce the ^{19}F CSA in the indirect dimension, but the symmetry numbers must be carefully chosen in order to avoid high rf amplitudes and care must be taken to avoid aliasing the broad recoupled patterns owing to the relatively large shift anisotropy. A $\mathrm{R12}_5^4$ sequence was found to be an appropriate choice for measuring ^{19}F shift parameters at ultrafast MAS rates. The new experiment was shown to be particularly useful for samples containing several inequivalent ^{19}F nuclei, with moderate ^{19}F CSAs (below 200 ppm at 600 MHz) and relatively small ^{1}H – ^{19}F dipolar couplings (below 10 kHz). As an example, the experiment was used to measure the ^{19}F shift parameters for the five sites that appear in the ^{19}F MAS spectrum of as-polymerized PVDF powder. Where the ^{19}F CSA (or the B_0 field) is larger an analysis of the spinning sidebands in the {^{1}H} – ^{19}F MAS spectrum is a more straightforward alternative to the method proposed here. In addition, it has been shown that applying a $\mathrm{R16}_3^2$ sequence to ^{1}H is an effective method of measuring H – F distances from the recoupled lineshapes which are sensitive to both the ^{1}H shift parameters and the ^{1}H – ^{19}F dipolar couplings.

Acknowledgments

HKM thanks the EPSRC and the University of Nottingham for a PhD studentship. The UK 850 MHz solid-state NMR Facility was funded by EPSRC and BBSRC, as well as the University of Warwick, including part funding through Birmingham Science City Advanced Materials Projects 1 and 2, supported by Advantage West Midlands (AWM) and the European Regional Development Fund (ERDF). We are grateful to F. Costantino and M. Taddei (Perugia) for providing the zirconium phosphonate.

References

1. D. H. Brouwer and J. A. Ripmeester, *J. Magn. Reson.*, 2007, **185**, 173–178.
2. M. Carravetta, M. Eden, X. Zhao, A. Brinkmann, and M. H. Levitt, *Chem. Phys. Lett.*, 2000, **321**, 205–215.

3. M. H. Levitt, *J. Chem. Phys.*, 2008, **128**, 052205.
4. G. Hou, S. Paramasivam, S. Yan, T. Polenova, and A. J. Vega, *J. Am. Chem. Soc.*, 2013, **135**, 1358–1368.
5. H. K. Miah, D. A. Bennett, D. Iuga, and J. J. Titman, *J. Magn. Reson.*, 2013, **235**, 1–5.
6. L. Duma, D. Abergel, P. Tekely, and G. Bodenhausen, *Chem. Commun.*, 2008, 2361.
7. J. Herzfeld and A. E. Berger, *J. Chem. Phys.*, 1980, **73**, 6021–6030.
8. R. K. Harris and P. Jackson, *Chem. Rev.*, 1991, **91**, 1427–1440.
9. U. Scheler and R. K. Harris, *Chem. Phys. Lett.*, 1996, **262**, 137–141.
10. M. Mehring, R. G. Griffin, and J. S. Waugh, *The Journal of Chemical Physics*, 1971, **55**, 746–755.
11. M. H. Levitt, *Symmetry-Based Pulse Sequences in Magic-Angle Spinning Solid-State NMR*, in *Encyclopedia of Magnetic Resonance*, Eds.-in-chief R. K. Harris and R. Wasylishen, John Wiley & Sons, Ltd, Chichester, UK, 2007.
12. G. Hou, I.-J. L. Byeon, J. Ahn, A. M. Gronenborn, and T. Polenova, *J. Am. Chem. Soc.*, 2011, **133**, 18646–18655.
13. A. Brinkmann and M. H. Levitt, *J. Chem. Phys.*, 2001, **115**, 357.
14. M. Bak, J. T. Rasmussen, and N. C. Nielsen, *J. Magn. Reson.*, 2000, **147**, 296–330.
15. S. K. Zaremba, *Ann. Mat. Pura. Appl.*, 1966, **73**, 293–317.
16. W. T. Eadie, D. Drijard, F. E. James, M. Roos, and B. Sadoulet, *Statistical Methods in Experimental Physics*, North Holland Publishing Co., Amsterdam, 1971.
17. S. Ando, R. K. Harris, and S. A. Reinsberg, *Magn. Reson. Chem.*, 2002, **40**, 97–106.
18. P. Holstein, R. K. Harris, and B. J. Say, *Solid State Nucl. Magn. Reson.*, 1997, **8**, 201–206.
19. C. Hucher, F. Beaume, R.-P. Eustache, and P. Tekely, *Macromolecules*, 2005, **38**, 1789–1796.
20. B. R. McGarvey and S. Schlick, *Macromolecules*, 1984, **17**, 2392–2399.
21. M. A. Bachmann and J. B. Lando, *Macromolecules*, 1981, **14**, 40–46.
22. F. Costantino, P. Sassi, M. Geppi, and M. Taddei, *Cryst. Growth Des.*, 2012, **12**, 5462–5470.